

# UC Berkeley

## UC Berkeley Previously Published Works

### Title

Chemical State Evolution in Ferroelectric Films during Tip-Induced Polarization and Electroresistive Switching

### Permalink

<https://escholarship.org/uc/item/1472k706>

### Journal

ACS Applied Materials & Interfaces, 8(43)

### ISSN

1944-8244

### Authors

levlev, Anton V  
Maksymovych, Petro  
Trassin, Morgan  
[et al.](#)

### Publication Date

2016-11-02

### DOI

10.1021/acsami.6b10784

Peer reviewed

# Chemical State Evolution in Ferroelectric Films during Tip-Induced Polarization and Electroresistive Switching

Anton V. Ievlev,<sup>\*,†,‡</sup> Petro Maksymovych,<sup>†,‡</sup> Morgan Trassin,<sup>§,||</sup> Jan Seidel,<sup>§,⊥</sup> Ramamoorthy Ramesh,<sup>§</sup> Sergei V. Kalinin,<sup>†,‡</sup> and Olga S. Ovchinnikova<sup>\*,†,‡</sup>

<sup>†</sup>The Center for Nanophase Materials Sciences, Oak Ridge National Laboratory, 1 Bethel Valley Rd., Oak Ridge, Tennessee 37831, United States

<sup>‡</sup>Institute for Functional Imaging of Materials, Oak Ridge National Laboratory, 1 Bethel Valley Rd., Oak Ridge, Tennessee 37831, United States

<sup>§</sup>Materials Sciences Division, Lawrence Berkeley National Laboratory, Berkeley, California 94720, United States

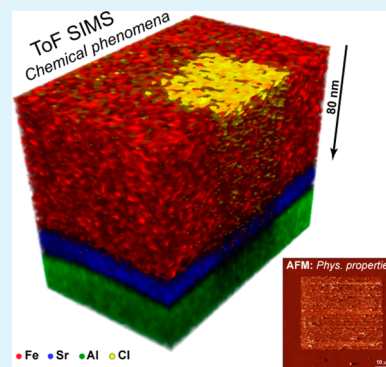
<sup>||</sup>Department of Materials, ETH Zurich, Vladimir-Prelog-Weg 4, 8093 Zurich, Switzerland

<sup>⊥</sup>School of Materials Science and Engineering, University of New South Wales, Sydney New South Wales 2052, Australia

## S Supporting Information

**ABSTRACT:** Domain formation and ferroelectric switching is fundamentally inseparable from polarization screening, which on free surfaces can be realized via band bending and ionic adsorption. In the latter case, polarization switching is intrinsically coupled to the surface electrochemical phenomena, and the electrochemical stage can control kinetics and induce long-range interactions. However, despite extensive evidence toward the critical role of surface electrochemistry, little is known about the nature of the associated processes. Here we combine SPM tip induce polarization switching and secondary ion mass spectrometry to explore the evolution of chemical state of ferroelectric during switching. Surprisingly, we find that even pristine surfaces contain ions (e.g., Cl<sup>-</sup>) that are not anticipated based on chemistry of the system and processing. In the ferroelectric switching regime, we find surprising changes in surface chemistry, including redistribution of base cations. At higher voltages in the electroforming regime significant surface deformation was observed and associated with a strong ion intermixing.

**KEYWORDS:** ferroelectric thin film, polarization switching, atomic force microscopy, time-of-flight secondary ion mass spectrometry, chemical phenomena, ion intermixing



## INTRODUCTION

Scanning probe microscopy (SPM) has become a standard tool for characterization of ferroelectric materials on the nanoscale. Its multiple imaging modes allow for comprehensive investigations of almost all aspects of ferroelectric single crystals and thin films, including domain structures,<sup>1–6</sup> optical responses,<sup>7–9</sup> conductivity,<sup>10–12</sup> and surface potential.<sup>13–15</sup> In particular, piezoresponse force microscopy (PFM) can be used for static domain structure imaging on a sample surface with nanometer spatial resolution.<sup>1,16–19</sup> Moreover, the electric field produced by a conductive SPM tip can induce local polarization switching, enabling fundamental investigations of polarization dynamics and practical applications including nanostructure fabrication, data storage, and ferroelectric lithography.<sup>20–24</sup>

In the vast majority of experimental and theoretical work, polarization switching is analyzed with the implicit assumption of unchanged stoichiometry of chemical elements and the driving force given by the volume integral of polarization-electric field product.<sup>25–30</sup> However, it is well recognized that even bulk polarization is unstable unless it is screened at the surfaces, by either metallic electrodes, band bending,<sup>31,32</sup> or

surface ionic charges.<sup>33–35</sup> The broad spectrum of phenomena including remnant potentials above Curie temperature,<sup>36,37</sup> temperature induced surface potential inversion,<sup>38</sup> shadowing of moving walls,<sup>39</sup> intermittency and chaos during polarization switching,<sup>23,40</sup> can be directly traced to the ionic screening charge dynamics.<sup>34</sup> Recently, a seminal work of synchrotron X-ray scattering has delivered insight into chemically controlled domain structure evolution, polarization switching, as well as provided direct evidence toward ionic screening on near-equilibrium surfaces.<sup>33,35,41–44</sup> However, tip-induced polarization switching is often performed under conditions (bias, times) that are known to result in a broad spectrum of electrochemical phenomena, including nano-oxidation or ionic motion.<sup>45–49</sup> Hence, these considerations suggest that the tip induced polarization switching may be strongly coupled to surface and even bulk electrochemical phenomena.

**Received:** August 29, 2016

**Accepted:** October 11, 2016

**Published:** October 11, 2016

Notably, the SPM does not provide direct ways for identification of chemical processes under the tip and even more so in the bulk. Therefore, all explorations to date have been done by either interpretation of secondary phenomena (e.g., electric potential change or domain structure evolution) or analyzing data of concomitant spectroscopic techniques (e.g., Raman scattering, Second Harmonic Generation,<sup>50</sup> X-ray scattering). At same time, secondary ion mass spectrometry (SIMS)<sup>51</sup> is able to provide spatially resolved information about chemical composition in a studied sample as a function of depth, offering a natural pathway to explore chemical changes on ferroelectric surface and bulk induced by locally applied SPM tip bias. This information can further be used for investigating the chemical and physical phenomena associated with polarization reversal in ferroelectrics.

Here, we employed time-of-flight secondary ion mass spectrometry (TOF-SIMS) to explore surface and bulk modifications in chemical composition and crystallographic structure of bismuth ferrite ferroelectric thin films induced by the local electric field of the SPM tip in the switching and electroforming regimes. Surprisingly, we found strong coupling between polarization and electroresistive switching and changes in surface chemistry, as well as a nontrivial serendipitous of surface chemistry on pristine surfaces. Understanding these phenomena is important for fundamental investigations of ferroelectric materials and has the potential to lead to the development of new practical applications of tip-mediated electrochemical reactions and material doping.

## EXPERIMENT AND RESULTS

In our experiments we used 80 nm thick thin film of BiFeO<sub>3</sub> doped with Ca, grown on La<sub>0.5</sub>Sr<sub>0.5</sub>CoO<sub>3</sub>/LaAlO<sub>3</sub> substrate as a model material with known ferroelectric properties.<sup>52</sup> SPM tip-induced electric field was used to produce changes in the thin-film stack of BFO/LSCO/LAO from pure ferroelectric polarization switching to electroforming and bias-induced degradation.

Initially, we used contact mode atomic force microscopy (AFM) and PFM to establish possible changes of the sample structure and define corresponding limits of applied biases. Specifically, we applied a switching voltage  $U_{sw}$  ranging from  $-100$  V to  $+100$  V between the bottom electrode and the conductive SPM tip while scanning square regions of  $20 \times 20$   $\mu\text{m}$  and  $40 \times 40$   $\mu\text{m}$  (Figure 1). Depending on the amplitude and polarity of applied bias, two types of associated changes were observed. First, polarization switching was observed during the application of relatively low negative voltages  $U_{sw} \sim -10$  V. Switching in this bias interval did not change sample surface and hence this low-voltage regime is referred as a ferroelectric switching mode. Ferroelectric switching has not been observed by positive voltage, since this is nonswitching direction for pristine polarization direction.

Increasing the voltage amplitude above 50 V showed significant irreversible changes in the surface topography of the modified region (average roughness above 40 nm) and sharp decrease in the piezoresponse signal (Figure 1 for  $-50$ ,  $-75$ , and  $-100$  V). Such a change in properties shows that the modified region has been irreversibly damaged, and does not show polar properties anymore. Additional measurements by conductive AFM tip demonstrated significant growth in its electro-conductivity (measured by the tip resistivity decreased down to 35 M $\Omega$ ; see Supporting Information Figure S1). Here and below this high-voltage regime is referred as a “electro-

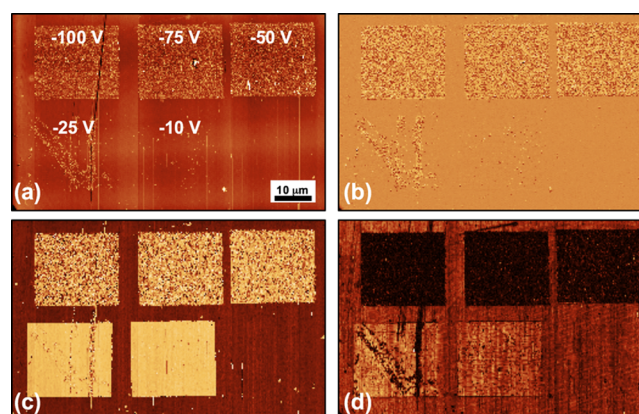


**Figure 1.** Tip-induced modification of BFO sample surface, measured by SPM. (a) AFM topography, (b) deflection, (c) PFM amplitude, and (d) PFM phase signals.

resistive”. Finally, application of the voltages in the intermediate range (between switching electro-resistive) led to spatial coexistence of low-field ferroelectric and high-field structural changes (Figure 1  $-25$  V).

To study structural and composition changes induce by biased tip, we prepared larger test areas of  $40 \times 40$   $\mu\text{m}$  squares modified in both switching ( $U_{sw} = \pm 10$  V) and electro-resistive ( $U_{sw} = \pm 100$  V) modes (Figure 2a,b). Note that polling by

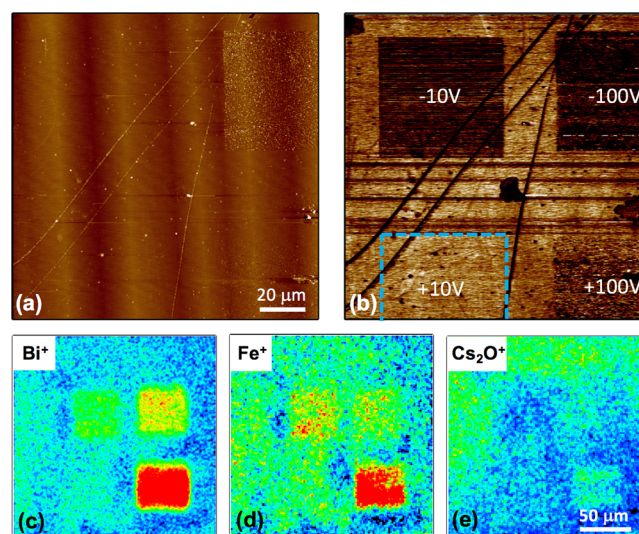


**Figure 2.** Detailed imaging of modified BFO surface. (a) AFM topography; (b) PFM amplitude; (c–e) Ions concentrations on the sample surface, measured by TOF-SIMS: (c) Bi<sup>+</sup>, (d) Fe<sup>+</sup>, and (e) Cs<sub>2</sub>O<sup>+</sup>.

$+10$  V did not lead to any observable changes, as ferroelectric switching was detected for negative voltages only, while the other three regions clearly demonstrate changes in either surface topography (Figure 1a,b) or PFM signals (Figure 1c,d).

TOF-SIMS measurements allowed direct measurements of the associated changes in chemical composition. Here, the TOF-SIMS experiments were optimized for the detection of the positive secondary ions, which allowed detection of the base components of BFO film and LSCO/LAO substrate, namely: Bi<sup>+</sup>, Fe<sup>+</sup>, Sr<sup>+</sup>, La<sup>+</sup>, and Al<sup>+</sup> ions (See details in Supporting Information Figure S2). However, measurements in this mode did not allow direct identification of the negatively charged ions

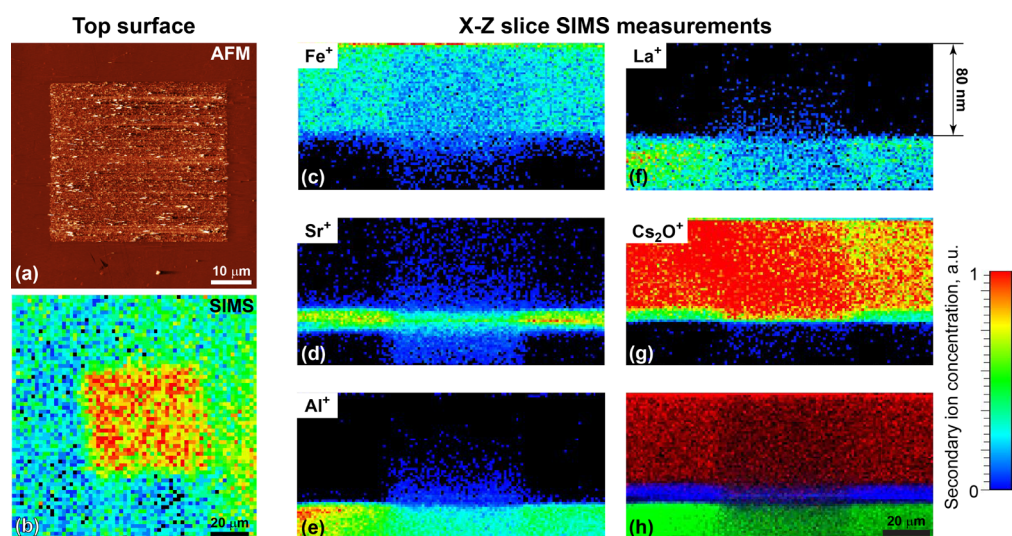


**Figure 3.** Region modified in electro-resistive mode. Top surface (a) AFM topography and (b) Secondary Bi<sup>+</sup> ions distribution. (c–g) XZ depth profiles of secondary ion concentrations: (c) Fe<sup>+</sup>; (d) Sr<sup>+</sup>; (e) Al<sup>+</sup>; (f) La<sup>+</sup>; (g) Cs<sub>2</sub>O<sup>+</sup>; (h) overlay of Fe<sup>+</sup> (red), Sr<sup>+</sup> (green) and Al<sup>+</sup> (blue).

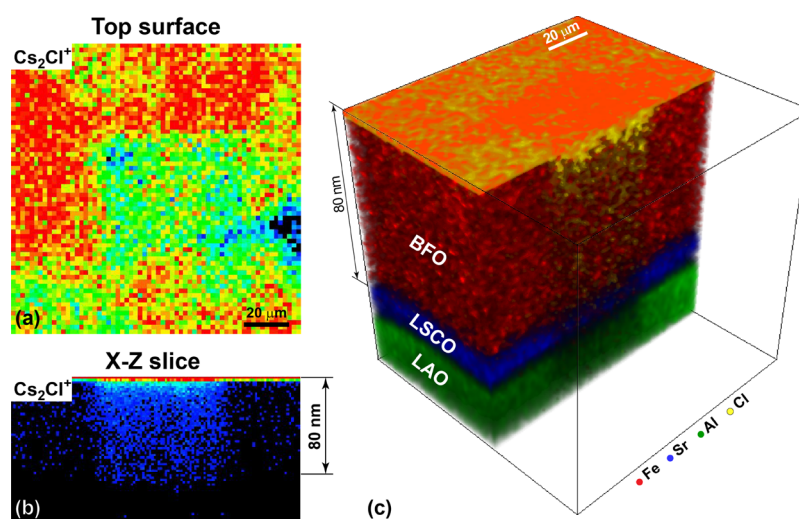


**Figure 4.** Spatial distributions of chloride ions on the film surface (a) and in the bulk (b), detected via Cs<sub>2</sub>Cl<sup>+</sup> clusters. (c) 3-dimensions overlay of Fe<sup>+</sup> (red), Sr<sup>+</sup> (blue), Al<sup>+</sup> (green) and Cs<sub>2</sub>Cl<sup>+</sup> (yellow) ions.

(e.g., oxygen, O<sup>-</sup> ions). To address this, we used Cs<sup>+</sup> ion gun as a sputtering source to create Cs clusters with the electro-negative ion and subsequently monitored for Cs<sub>2</sub>O<sup>+</sup> clusters. This also led to the preferential clustering of Bi<sup>+</sup> into a CsBi<sup>+</sup> clusters hampered the detection of pure Bi<sup>+</sup> ions in the film bulk, where CsBi<sup>+</sup> clusters were mostly detected (Supporting Information Figure S3c,d). Thereby, we used Bi<sup>+</sup> maps for analysis of the surface behavior only and CsBi<sup>+</sup> cluster maps to control the bulk.

TOF-SIMS measurements in a pristine BFO sample showed expected depth profiles of base elements, where Fe<sup>+</sup> was found in BFO film only; Sr<sup>+</sup> and La<sup>+</sup> – in LSCO layer; Al<sup>+</sup> and La<sup>+</sup> – in LAO substrate (Supporting Information Figure S3a). However, in addition to base elements of film and substrate pronounced amount of chlorine ions (detected by presence of Cs<sub>2</sub>Cl<sup>+</sup> ionic clusters) was found on the film surface (Supporting Information Figure S4a).

Similarly, we investigated changes in chemical composition induced by the SPM tip on the film surface (Figure 2) and in the bulk (Figure 3). In the case of ferroelectric switching (low-

voltage mode) surface scans showed up to 20% of Fe<sup>+</sup> and Bi<sup>+</sup> concentration increase (Figure 2c,d –10 V region). This behavior can be attributed to cation motion in a thin surface layer. Although, switching in this mode does not lead to observable surface topography changes (Figure 2a), tip-induced electric field in the thin surface layer exceeds 100 kV/mm,<sup>29</sup> which is enough to cause Fe<sup>+</sup> and Bi<sup>+</sup> redistribution.

Investigations in the regions modified in electro-resistive mode similarly showed increase of Bi<sup>+</sup> and Fe<sup>+</sup> concentrations on the sample surface (Figure 2c,d ± 100 V regions). Notably, both polarities of applied bias demonstrated growth of the surface Bi<sup>+</sup> and Fe<sup>+</sup> concentrations. This fact cannot be explained in terms of electrostatic phenomena only, as in this case electrostatic repulsive force should lead to depletion of the positive ions in the modified region. However, our experiments, showed completely opposite results –Bi<sup>+</sup> and Fe<sup>+</sup> concentrations are higher in the case of the positive bias. There can be different explanations of this unexpected behavior. First of all, it can have purely technical origin—electro-resistive switching showed significant changes in the surface topography, which is

most likely followed by the film amorphization and consequent increase in the efficiency of the secondary ion generation. This would explain sharp increase in the measured concentration of the secondary  $\text{Fe}^+$  and  $\text{Bi}^+$  ions, which however does not correspond to their actual concentration on the sample surface. At the same time, this explanation cannot be used for changes observed in the case of ferroelectric switching, as it does not show change in the sample topography (Figure 2a). Second, observed behavior can be a result of an electrochemical reaction, induced by the highly localized electric field in the presence of the top water layer.

In addition to surface changes, electro-resistive switching also showed significant changes in chemical composition in the film the bulk. To get further insight into those changes we performed detailed TOF-SIMS measurement on the freshly modified by  $U_{\text{sw}} = -100$  V region of  $40 \times 40 \mu\text{m}$  (Figure 3a,b). Detailed analysis of the depth profiles revealed significant cation intermixing (Figure 3), leading to penetration of  $\text{Fe}^+$  into LSCO layer and LAO substrate (Figure 3c) and vice versa –  $\text{Sr}^+$  (Figure 3d),  $\text{Al}^+$  (Figure 3e), and  $\text{La}^+$  (Figure 3f) penetrated deeply into the film. Introduction of the positive  $\text{Sr}^+$ ,  $\text{Al}^+$  and  $\text{La}^+$  ions form LSCO and LAO into the film as well as higher surface concentration of  $\text{Bi}^+$  and  $\text{Fe}^+$  can be easily explained by electrostatic attraction to a negatively biased tip. While opposite motion of  $\text{Fe}^+$  and  $\text{Sr}^+$  into LAO substrate, evidently has diffusional origin or associated with spatial inhomogeneity of the electric field near the LSCO layer.

As was already discussed TOF-SIMS revealed presence of the chlorine on the film surface. Investigations in modified region showed changes of  $\text{Cl}^-$  concentrations both on the surface (Figure 4a) and in the bulk (Figure 4b, Supporting Information Figure S4b). While chlorine concentration on the surface decreased, it was found to penetrate deeply into the film (Figure 4b,c), which agrees with a polarity of applied electric field. Negatively charged  $\text{Cl}^-$  and  $\text{O}^-$  ions repulse from the tip, producing depletion region on the sample surface and injecting deep into the film bulk. This explanation is confirmed by the spatial distribution of the  $\text{O}^-$  (Figure 2e) and  $\text{Cl}^-$  (Supporting Information Figure S5) on the surface of the region modified by positive bias.

These results suggest that tip-controlled polarization and electroresistive switching are both associated with the penetration of ions from the adsorption surface layer into the sample. Implications of these results are important for both fundamental studies of tip-induced phenomena in ferroics and wider range of materials and potentially open new direction of local material modification by surface and bulk electrochemistry mediated by the SPM tip.

## CONCLUSION

In conclusion, we investigated changes in the chemical composition of a ferroelectric bismuth ferrite thin-film introduced by a strongly inhomogeneous electric field. In our studies we used the biased tip of the scanning probe microscope to induce two types of surface and bulk changes: ferroelectric switching by application of relatively low electric fields and irreversible electro-resistive surface modification by application of higher fields. Correlative measurements of the biased areas by TOF-SIMS allowed investigation of associate changes in surface and bulk chemistry.

These measurements demonstrated a number of nontrivial phenomena. In particular, significant role of the serendipitous surface chemistries was confirmed by pronounced concen-

tration of chlorine ions on the sample surface and its penetration into the bulk of the modified region. Significant role of surface electrochemistry in the process of ferroelectric switching was justified by strong changes in the surface chemistry (concentrations of  $\text{Fe}^+$  and  $\text{Bi}^+$  ions). Finally, in the case of electro-resistive modification of surface and bulk cation intermixing was found to lead to the penetration of the  $\text{Sr}^+$ ,  $\text{La}^+$ ,  $\text{Al}^+$  ions from substrate into the film due to electrostatic attraction to the tip.

The phenomena explored in this paper are important from both fundamental and practical points of view. In particular, they confirm the significant role of electrochemistry on ferroelectric switching processes and its special role of adsorption surface layer. They also enable a number of practical applications for local material modifications and electrochemical processes controlled by the SPM tip.

## METHODS

**Studied Samples.** In our measurements, we used ferroelectric 80 nm thick thin film of bismuth ferrite  $\text{BiFeO}_3$  (BFO) doped with 2% of Ca and grown on  $\text{LaAlO}_3$  (LAO) dielectric substrate with 10 nm layer of  $\text{La}_{0.5}\text{Sr}_{0.5}\text{CoO}_3$  (LSCO). Details of the growth procedure can be found in ref<sup>52</sup>.

**Atomic Force Microscopy.** AFM and PFM measurement were performed by Ntegra Spectra (NT-MDT, Russia) scanning probe microscope using Multi-75 Pt-coated tips (Budget Sensors). For film surface modification voltage  $U_{\text{sw}} = -100$ – $100$  V was applied between tip and bottom electrode.

**Time-of-Flight Secondary Ion Mass Spectrometry.** Mass spectrometry measurements were performed in positive ions detection mode using TOF SIMS-5 (ION-TOF GmbH, Germany) using a 30 keV Bi ion gun as the primary gun with a focused ion beam spot size of  $\sim 5 \mu\text{m}$ , and a  $m/\Delta m$  resolution of  $5000 \div 11\,000$ . The images were collected with a resolution of  $256 \times 256$  points across a  $129$  and  $200 \mu\text{m}$  imaging areas. Depth profiling of the sample was carried out using a  $\text{Cs}^+$  ion-sputtering source operated at 1 keV and 50 nA, and sputtering for 10 s per slice over a  $300 \mu\text{m}$  total area. The 3D data was reconstructed from 65 depth profile scans that corresponds to a depth of  $\sim 2.5$  nm per image slice. The data was collected in positive ion mode with Cl and O forming  $\text{Cs}_2\text{Cl}^+$  and  $\text{Cs}_2\text{O}^+$  clusters.

## ASSOCIATED CONTENT

### Supporting Information

The Supporting Information is available free of charge on the ACS Publications website at DOI: 10.1021/acsami.6b10784.

Detailed information on current measurements and ToF SIMS (PDF)

## AUTHOR INFORMATION

### Corresponding Authors

\*(A.V.I.) E-mail: ievlevav@ornl.gov.

\*(O.S.O.) E-mail: ovchinnikovo@ornl.gov.

### Author Contributions

A.V.I. has obtained and analyzed the experimental data. M.T., J.S., and R.R. grew and provided BFO thin films. All authors wrote and edited paper. O.S.O. and S.V.K. directed the research.

### Notes

The authors declare no competing financial interest.

## ACKNOWLEDGMENTS

This material is based upon work supported by the U.S. Department of Energy, Office of Science, Office of Basic Energy Sciences under contract number DE-AC05-00OR22725.

Interpretation of BFO ferroelectric switching was conducted at the Center for Nanophase Materials Sciences, which is a DOE Office of Science User Facility (PM), the understanding of ion mixing and ionic motion in BFO was supported by Division of Materials Sciences and Engineering Division, Office of Basic Energy Sciences, development of AFM/SIMS approach for understanding electromechanical motion in ferroelectrics was supported U.S. DOE (SVK), and by the Laboratory Directed Research and Development Program of Oak Ridge National Laboratory, managed by UT-Battelle, LLC, for the U. S. Department of Energy (AVI, OSO).

## REFERENCES

- (1) Kalinin, S. V.; Morozovska, A. N.; Chen, L. Q.; Rodriguez, B. J. Local Polarization Dynamics in Ferroelectric Materials. *Rep. Prog. Phys.* **2010**, *73*, 056502.
- (2) Gruverman, A.; Auciello, O.; Tokumoto, H. Scanning Force Microscopy for the Study of Domain Structure in Ferroelectric Thin Films. *J. Vac. Sci. Technol., B: Microelectron. Process. Phenom.* **1996**, *14*, 602–605.
- (3) Soergel, E. Piezoresponse Force Microscopy (PFM). *J. Phys. D: Appl. Phys.* **2011**, *44*, 464003.
- (4) Hong, S.; Tong, S.; Park, W. I.; Hiranaga, Y.; Cho, Y. S.; Roelofs, A. Charge Gradient Microscopy. *Proc. Natl. Acad. Sci. U. S. A.* **2014**, *111*, 6566–6569.
- (5) Tong, S.; Jung, I. W.; Choi, Y. Y.; Hong, S.; Roelofs, A. Imaging Ferroelectric Domains and Domain Walls Using Charge Gradient Microscopy: Role of Screening Charges. *ACS Nano* **2016**, *10*, 2568–2574.
- (6) Denning, D.; Guyonnet, J.; Rodriguez, B. J. Applications of Piezoresponse Force Microscopy in Materials Research: From Inorganic Ferroelectrics to Biopiezoelectrics and Beyond. *Int. Mater. Rev.* **2016**, *61*, 46–70.
- (7) Ievlev, A. V.; Susner, M. A.; McGuire, M. A.; Maksymovych, P.; Kalinin, S. V. Quantitative Analysis of the Local Phase Transitions Induced by Laser Heating. *ACS Nano* **2015**, *9*, 12442–12450.
- (8) Lipatov, A.; Sharma, P.; Gruverman, A.; Sinitiskii, A. Optoelectrical Molybdenum Disulfide (MoS<sub>2</sub>)-Ferroelectric Memories. *ACS Nano* **2015**, *9*, 8089–8098.
- (9) Pingree, L. S. C.; Reid, O. G.; Ginger, D. S. Electrical Scanning Probe Microscopy on Active Organic Electronic Devices. *Adv. Mater.* **2009**, *21*, 19–28.
- (10) Seidel, J.; Martin, L. W.; He, Q.; Zhan, Q.; Chu, Y. H.; Rother, A.; Hawkrige, M. E.; Maksymovych, P.; Yu, P.; Gajek, M.; Balke, N.; Kalinin, S. V.; Gemming, S.; Wang, F.; Catalan, G.; Scott, J. F.; Spaldin, N. A.; Orenstein, J.; Ramesh, R. Conduction at Domain Walls in Oxide Multiferroics. *Nat. Mater.* **2009**, *8*, 229–234.
- (11) Kim, Y.-M.; Morozovska, A.; Eliseev, E.; Oxley, M. P.; Mishra, R.; Selbach, S. M.; Grande, T.; Pantelides, S. T.; Kalinin, S. V.; Borisevich, A. Y. Direct Observation of Ferroelectric Field Effect and Vacancy-controlled Screening at the BiFeO<sub>3</sub>/La<sub>x</sub>Sr<sub>1-x</sub>MnO<sub>3</sub> interface. *Nat. Mater.* **2014**, *13*, 1019–1025.
- (12) Crassous, A.; Sluka, T.; Tagantsev, A. K.; Setter, N. Polarization Charge as a Reconfigurable Quasi-Dopant In Ferroelectric Thin Films. *Nat. Nanotechnol.* **2015**, *10*, 614.
- (13) Haussmann, A.; Milde, P.; Erler, C.; Eng, L. M. Ferroelectric Lithography: Bottom-up Assembly and Electrical Performance of a Single Metallic Nanowire. *Nano Lett.* **2009**, *9*, 763–768.
- (14) Kim, Y.; Bae, C.; Ryu, K.; Ko, H.; Kim, Y. K.; Hong, S.; Shin, H. Origin of Surface Potential Change During Ferroelectric Switching in Epitaxial PbTiO<sub>3</sub> Thin Films Studied by Scanning Force Microscopy. *Appl. Phys. Lett.* **2009**, *94*, 032907.
- (15) Kalinin, S. V.; Bonnell, D. A. Local Potential and Polarization Screening on Ferroelectric Surfaces. *Phys. Rev. B: Condens. Matter Mater. Phys.* **2001**, *63*, 125411.
- (16) Bonnell, D. A.; Kalinin, S. V.; Kholkin, A. L.; Gruverman, A. Piezoresponse Force Microscopy: A Window into Electromechanical Behavior at the Nanoscale. *MRS Bull.* **2009**, *34*, 648–657.
- (17) Gruverman, A.; Kholkin, A. Nanoscale Ferroelectrics: Processing, Characterization and Future Trends. *Rep. Prog. Phys.* **2006**, *69*, 2443–2474.
- (18) Balke, N.; Bdiqin, I.; Kalinin, S. V.; Kholkin, A. L. Electromechanical Imaging and Spectroscopy of Ferroelectric and Piezoelectric Materials: State of the Art and Prospects for the Future. *J. Am. Ceram. Soc.* **2009**, *92*, 1629–1647.
- (19) Kalinin, S. V.; Rar, A.; Jesse, S. A Decade of Piezoresponse Force Microscopy: Progress, Challenges, and Opportunities. *IEEE Trans. Ultrason. Eng.* **2006**, *53*, 2226–2252.
- (20) Hatanaka, T.; Nakamura, K.; Taniuchi, T.; Ito, H.; Furukawa, Y.; Kitamura, K. Quasi-Phase-matched Optical Parametric Oscillation with Periodically Poled Stoichiometric LiTaO<sub>3</sub>. *Opt. Lett.* **2000**, *25*, 651–653.
- (21) Cho, Y.; Fujimoto, K.; Hiranaga, Y.; Wagatsuma, Y.; Onoe, A.; Terabe, K.; Kitamura, K. Tbit/inch<sup>2</sup> Ferroelectric Data Storage Based on Scanning Nonlinear Dielectric Microscopy. *Appl. Phys. Lett.* **2002**, *81*, 4401.
- (22) Ievlev, A. V.; Kalinin, S. V. Data Encoding Based on the Shape of the Ferroelectric Domains Produced by Using a Scanning Probe Microscope Tip. *Nanoscale* **2015**, *7*, 11040–11047.
- (23) Ievlev, A. V.; Jesse, S.; Morozovska, A. N.; Strelcov, E.; Eliseev, E. A.; Pershin, Y. V.; Kumar, A.; Shur, V. Y.; Kalinin, S. V. Intermittency, Quasiperiodicity and Chaos in Probe-Induced Ferroelectric Domain Switching. *Nat. Phys.* **2014**, *10*, 59–66.
- (24) Scott, J. F. Applications of Modern Ferroelectrics. *Science* **2007**, *315*, 954–959.
- (25) Molotskii, M. Generation of Ferroelectric Domains in Atomic Force Microscope. *J. Appl. Phys.* **2003**, *93*, 6234–6237.
- (26) Agronin, A.; Molotskii, M.; Rosenwaks, Y.; Rosenman, G.; Rodriguez, B. J.; Kingon, A. I.; Gruverman, A. Dynamics of Ferroelectric Domain Growth in the Field of Atomic Force Microscope. *J. Appl. Phys.* **2006**, *99*, 104102.
- (27) Morozovska, A. N.; Kalinin, S. V.; Eliseev, E. A.; Gopalan, V.; Svechnikov, S. V. Interaction of a 180 Degrees Ferroelectric Domain Wall with a Biased Scanning Probe Microscopy Tip: Effective Wall Geometry and Thermodynamics in Ginzburg-Landau-Devonshire Theory. *Phys. Rev. B: Condens. Matter Mater. Phys.* **2008**, *78*, 125407.
- (28) Morozovska, A. N.; Eliseev, E. A.; Bravina, S. L.; Kalinin, S. V. Landau-Ginzburg-Devonshire Theory for Electromechanical Hysteresis Loop Formation in Piezoresponse Force Microscopy of Thin Films. *J. Appl. Phys.* **2011**, *110*, 052011.
- (29) Ievlev, A. V.; Morozovska, A. N.; Shur, V. Y.; Kalinin, S. V. Humidity Effects on Tip-Induced Polarization Switching in Lithium Niobate. *Appl. Phys. Lett.* **2014**, *104*, 092908.
- (30) Ievlev, A. V.; Alikin, D. O.; Morozovska, A. N.; Varenky, O. V.; Eliseev, E. A.; Kholkin, A. L.; Shur, V. Y.; Kalinin, S. V. Symmetry Breaking and Electrical Frustration during Tip-Induced Polarization Switching in the Nonpolar Cut of Lithium Niobate Single Crystals. *ACS Nano* **2015**, *9*, 769–777.
- (31) Fridkin, V. M.: *Ferroelectric Semiconductors*; Springer: New York, 1980.
- (32) Vul, B. M.; Guro, G. M.; Ivanchik, I. I. Encountering Domains in Ferroelectrics. *Ferroelectrics* **1973**, *6*, 29–31.
- (33) Wang, R. V.; Fong, D. D.; Jiang, F.; Highland, M. J.; Fuoss, P. H.; Thompson, C.; Kolpak, A. M.; Eastman, J. A.; Streiffer, S. K.; Rappe, A. M.; Stephenson, G. B. Reversible Chemical Switching of a Ferroelectric Film. *Phys. Rev. Lett.* **2009**, *102*, 047601.
- (34) Kalinin, S. V.; Bonnell, D. A. Screening Phenomena on Oxide Surfaces and its Implications for Local Electrostatic and Transport Measurements. *Nano Lett.* **2004**, *4*, 555–560.
- (35) Stephenson, G. B.; Highland, M. J. Equilibrium and Stability of Polarization in Ultrathin Ferroelectric Films with Ionic Surface Compensation. *Phys. Rev. B: Condens. Matter Mater. Phys.* **2011**, *84*, 064107.
- (36) Kalinin, S. V.; Bonnell, D. A. Characterization of Ferroelectric BaTiO<sub>3</sub> (100) Surfaces by Variable Temperature Scanning Surface Potential Microscopy and Piezoresponse Imaging. *MRS Online Proc. Libr.* **2000**, *596*, 327–332.

(37) Kalinin, S. V.; Bonnell, D. A. Effect of Phase Transition on the Surface Potential of the BaTiO<sub>3</sub> (100) Surface by Variable Temperature Scanning Surface Potential Microscopy. *J. Appl. Phys.* **2000**, *87*, 3950–3957.

(38) Kalinin, S. V.; Johnson, C. Y.; Bonnell, D. A. Domain Polarity and Temperature Induced Potential Inversion on the BaTiO<sub>3</sub>(100) Surface. *J. Appl. Phys.* **2002**, *91*, 3816–3823.

(39) Kalinin, S. V.; Bonnell, D. A. Local Potential and Polarization Screening on Ferroelectric Surfaces. *Phys. Rev. B: Condens. Matter Mater. Phys.* **2001**, *63*, 125411.

(40) Ievlev, A. V.; Morozovska, A. N.; Eliseev, E. A.; Shur, V. Y.; Kalinin, S. V. Ionic Field Effect and Memristive Phenomena in Single-Point Ferroelectric Domain Switching. *Nat. Commun.* **2014**, *5*, 5545.

(41) Highland, M. J.; Fister, T. T.; Fong, D. D.; Fuoss, P. H.; Thompson, C.; Eastman, J. A.; Streiffer, S. K.; Stephenson, G. B. Equilibrium Polarization of Ultrathin PbTiO<sub>3</sub> with Surface Compensation Controlled by Oxygen Partial Pressure. *Phys. Rev. Lett.* **2011**, *107*, 178602.

(42) Highland, M. J.; Fister, T. T.; Richard, M. I.; Fong, D. D.; Fuoss, P. H.; Thompson, C.; Eastman, J. A.; Streiffer, S. K.; Stephenson, G. B. Polarization Switching without Domain Formation at the Intrinsic Coercive Field in Ultrathin Ferroelectric PbTiO<sub>3</sub>. *Phys. Rev. Lett.* **2010**, *105*, 167601.

(43) Fong, D. D.; Kolpak, A. M.; Eastman, J. A.; Streiffer, S. K.; Fuoss, P. H.; Stephenson, G. B.; Thompson, C.; Kim, D. M.; Choi, K. J.; Eom, C. B.; Grinberg, I.; Rappe, A. M. Stabilization of Monodomain Polarization in Ultrathin PbTiO<sub>3</sub> Films. *Phys. Rev. Lett.* **2006**, *96*, 127601.

(44) Streiffer, S. K.; Eastman, J. A.; Fong, D. D.; Thompson, C.; Munkholm, A.; Murty, M. V. R.; Auciello, O.; Bai, G. R.; Stephenson, G. B. Observation of Nanoscale 180 Degree Stripe Domains in Ferroelectric PbTiO<sub>3</sub> Thin Films. *Phys. Rev. Lett.* **2002**, *89*, 067601.

(45) Garcia, R.; Knoll, A. W.; Riedo, E. Advanced Scanning Probe Lithography. *Nat. Nanotechnol.* **2014**, *9*, 577–587.

(46) Garcia, R.; Losilla, N. S.; Martinez, J.; Martinez, R. V.; Palomares, F. J.; Huttel, Y.; Calvaresi, M.; Zerbetto, F. Nanopatterning of Carbonaceous Structures by Field-Induced Carbon Dioxide Splitting with a Force Microscope. *Appl. Phys. Lett.* **2010**, *96*, 96.

(47) Garcia, R.; Martinez, R. V.; Martinez, J. Nano-chemistry and Scanning Probe Nanolithographies. *Chem. Soc. Rev.* **2006**, *35*, 29–38.

(48) Doria, S.; Yang, N.; Kumar, A.; Jesse, S.; Tebano, A.; Aruta, C.; Di Bartolomeo, E.; Arruda, T. M.; Kalinin, S. V.; Licoccia, S.; Balestrino, G. Nanoscale Mapping of Oxygen Vacancy Kinetics in Nanocrystalline Samarium Doped Ceria Thin Films. *Appl. Phys. Lett.* **2013**, *103*, 171605.

(49) Kumar, A.; Ciucci, F.; Morozovska, A. N.; Kalinin, S. V.; Jesse, S. Measuring Oxygen Reduction/Evolution Reactions on the Nanoscale. *Nat. Chem.* **2011**, *3*, 707–713.

(50) Trassin, M.; De Luca, G.; Manz, S.; Fiebig, M. Probing Ferroelectric Domain Engineering in BiFeO<sub>3</sub> Thin Films by Second Harmonic Generation. *Adv. Mater.* **2015**, *27*, 4871–4876.

(51) McDonnell, L. A.; Heeren, R. M. A. Imaging Mass Spectrometry. *Mass Spectrom. Rev.* **2007**, *26*, 606–643.

(52) Seidel, J.; Trassin, M.; Zhang, Y.; Maksymovych, P.; Uhlig, T.; Milde, P.; Kohler, D.; Baddorf, A. P.; Kalinin, S. V.; Eng, L. M.; Pan, X. Q.; Ramesh, R. Electronic Properties of Isosymmetric Phase Boundaries in Highly Strained Ca-Doped BiFeO<sub>3</sub>. *Adv. Mater.* **2014**, *26*, 4376–4380.